PET of Malignant Melanoma Using ^{18}F-Labeled Metallopeptides

Gang Ren*[1], Zhe Liu*[1], Zheng Miao[1], Hongguang Liu[1], Murugesan Subbarayan[1], Frederick T. Chin[1], Lan Zhang[2], Sanjiv S. Gambhir[1], and Zhen Cheng[1]

[1]*Molecular Imaging Program at Stanford (MIPS), Department of Radiology and Bio-X Program, Stanford University, Stanford, California; and* [2]*Shanghai Institute of Applied Physics, Chinese Academy of Sciences, Shanghai, China*

Melanocortin type 1 receptor (MC1R), also known as α-melanocyte–stimulating hormone (α-MSH) receptor, is an attractive molecular target for melanoma imaging and therapy. An ^{18}F-labeled linear α-MSH peptide (^{18}F-FB-Ac-Nle-Asp-His-D-Phe-Arg-Trp-Gly-Lys-NH_2 [NAPamide]) shows promising melanoma imaging properties but with only moderate tumor uptake and retention. A transition metal rhenium-cyclized α-MSH peptide, ReO[Cys^{3,4,10},D-Phe^{7},Arg^{11}]α-$MSH_{3–13}$ (ReCCMSH(Arg^{11})), has shown high in vitro binding affinity to MC1R and excellent in vivo melanoma-targeting profiles when labeled with radiometals. Therefore, we hypothesized that ReCCMSH(Arg^{11}) could be a good platform for the further development of an ^{18}F-labeled probe for PET of MC1R-positive malignant melanoma. **Methods:** In this study, the metallopeptide Ac-D-Lys-ReCCMSH(Arg^{11}) was synthesized using conventional solid-phase peptide synthesis chemistry and a rhenium cyclization reaction. The resulting peptides were then labeled with *N*-succinimidyl-4-^{18}F-fluorobenzoate (^{18}F-SFB). The ^{18}F-labeled metallopeptides were further tested for their in vitro receptor binding affinities, in vivo biodistribution, and PET imaging properties. **Results:** Both isomers of Ac-D-Lys-ReCCMSH(Arg^{11}), named as RMSH-1 and RMSH-2, were purified and identified by high-performance liquid chromatography. The binding affinities of RMSH-1 and RMSH-2 and their respective ^{19}F-SFB–conjugated peptides (^{19}F-FB-RMSH-1 and ^{19}F-FB-RMSH-2) were all determined to be within nanomolar range. Both ^{18}F-labeled metallopeptides showed good tumor uptake in the B16F10 murine model, with high MC1R expression, but much lower uptake in the A375M human melanoma xenografted in mice, indicating low MC1R expression. ^{18}F-FB-RMSH-1, when compared with ^{18}F-FB-RMSH-2, displayed more favorable in vivo performance in terms of slightly higher tumor uptakes and much lower accumulations in the kidney and liver at 2 h after injection. Small-animal PET of ^{18}F-FB-RMSH-1 and -2 in mice bearing B16F10 tumors at 1 and 2 h showed good tumor imaging quality. As expected, much lower tumor uptakes and poorer tumor–to–normal organ contrasts were observed for the A375M model than for the B16F10 model. ^{18}F-FB-RMSH-1 and -2 showed higher tumor uptake and better tumor retention than did ^{18}F-FB-NAPamide. **Conclusion:** Specific in vivo targeting of ^{18}F-FB-RMSH-1 to malignant melanoma was successfully achieved in preclinical models with high MC1R expression. Thus, the radiofluorinated metallopeptide ^{18}F-FB-RMSH-1 is a promising molecular probe for PET of MC1R-positive tumors.

Key Words: malignant melanoma; α-MSH; PET; imaging; ^{18}F

J Nucl Med 2009; 50:1865–1872
DOI: 10.2967/jnumed.109.062877

Received Apr. 11, 2009; revision accepted Aug. 11, 2009.
For correspondence or reprints contact: Zhen Cheng, Molecular Imaging Program at Stanford, Department of Radiology and Bio-X Program, 1201 Welch Rd., Lucas Expansion, P020A, Stanford University, Stanford, CA 94305-5484.
E-mail: zcheng@stanford.edu
*Contributed equally to this work.

Malignant melanoma is still increasing. According to the National Cancer Institute, there will be an estimated 68,720 new cases and 8,650 deaths all over the United States in 2009. It is an aggressive disease with high metastatic potential and resistance to cytotoxic agents. Representing only 5% of all skin cancer types, melanoma contributes to more than 50% of deaths related to skin cancer (*1,2*).

Imaging techniques play crucial roles in diagnosing and staging cancers and individualizing treatment plans for patients. The earlier detection and staging of malignant melanoma is important for better management of the disease. ^{18}F-FDG PET provides useful information for the detection of distal organ metastases and has been widely used in the staging of malignant melanoma in the clinic (*3*). However, ^{18}F-FDG PET (*4,5*), 3′-^{18}F-fluoro-3′-deoxy-L-thymidine (*6*), and ^{18}F-galacto-arginine-glycine-aspartic acid (*7*) all have limitations in terms of sensitivity and specificity. Novel PET molecular probes are still in great demand to image specific melanoma-associated targets, detect melanoma micrometastases, and improve the current management.

Melanocortin type 1 receptor (MC1R) is a G-protein–coupled receptor and has been known to be overexpressed in many types of murine and human melanomas, making it an attractive target for receptor-based imaging and therapy (*8,9*). Its major ligand, α-melanocyte–stimulating hormone (α-MSH), is derived from a precursor hormone called proopiomelanocortin. Many α-MSH analogs have been synthesized, labeled with different radioisotopes, and reported to be highly selective to melanoma because of their high binding specificity to MC1R (*10–22*). Currently, 2 classes of α-MSH analogs have shown the most promising

results for the in vivo targeting of melanoma. The first one is transition metal rhenium-cyclized α-MSH, ReO[Cys^{3,4,10},D-Phe^{7},Arg^{11}]α-MSH$_{3–13}$ (referred to as ReCCMSH(Arg^{11}))–based analogs (*10,14,15,19,21,22*); the other is the linear α-MSH, Ac-Nle-Asp-His-D-Phe-Arg-Trp-Gly-Lys-NH_2 (referred to as NAPamide)–based peptides (*11,12,18,20*).

In our previous research, NAPamide has been labeled with a highly clinically relevant PET radioisotope, ^{18}F. The conjugation of *N*-succinimidyl-4-^{18}F-fluorobenzoate (^{18}F-SFB) through the lysine side chain ε-amino group in NAPamide generated a radiopeptide ^{18}F-FB-NAPamide (Fig. 1) (*11*). Further small-animal PET with this probe in tumor-bearing mice demonstrated that ^{18}F-FB-NAPamide could clearly detect MC1R-positive melanoma and differentiate melanomas with high and low MC1R expression. These earlier results highlight the potential use of an ^{18}F-labeled α-MSH peptide for clinical melanoma MC1R imaging. However, the associated biodistribution experiments showed that ^{18}F-FB-NAPamide displayed only moderate tumor uptake and retention (1.19 ± 0.11 and 0.25 ± 0.05 percentage injected dose per gram [%ID/g], respectively, in B16F10 xenografted melanoma at 1 and 4 h after injection). This phenomenon is usually caused by the rapid release of radioactivity from tumors after the internalization of radiohalogenated peptides (*19*). To develop an ^{18}F-labeled α-MSH analog that can be translated for clinical use, strategies are required to improve radiotracer uptake and retention in tumors.

ReCCMSH(Arg^{11}) and related analogs have demonstrated high in vivo tumor radioactivity uptake and long tumor cellular retention because of their high resistance to proteolytic degradation of this novel metallopeptide scaffold, which makes ReCCMSH(Arg^{11}) an ideal structural motif for the development of melanoma-targeting agents (*10,14,15,19,21,22*). Ac-D-Lys-ReCCMSH(Arg^{11}) (abbreviated as RMSH) was thus designed and conjugated with 4-^{125}I-iodobenzoate to produce Ac-D-Lys(^{125}I-IBA)-ReCCMSH(Arg^{11}) (abbreviated as ^{125}I-IB-RMSH) and showed decent tumor uptake in vivo (*19*). In this study, we hypothesized that a PET probe with good melanoma uptake and retention might be achieved by replacing ^{125}I with ^{18}F in an ^{125}I-IB-RMSH molecule. The ^{18}F-SFB–conjugated RMSH Ac-D-Lys(^{18}F-FB)-ReCCMSH(Arg^{11}) (abbreviated as ^{18}F-FB-RMSH, Fig. 1) was synthesized and further evaluated by PET for melanoma and MC1R expression in mice tumor models.

MATERIALS AND METHODS

General

^{125}I-(Tyr^{2})-[Nle^{4}, D-Phe^{7}]-α-MSH [^{125}I-(Tyr^{2})-NDP] was purchased from Perkin Elmer. All *N*-α-Fmoc–protected amino acids were purchased from Advanced Chemtech. Dimethylformamide and methylene chloride were from Fisher Scientific. Piperidine (20%) in dimethylformamide and 0.4 M *N*-methylmorpholine in dimethylformamide were from Protein Technologies Inc. Trifluoroacetic acid (TFA), *O*-benzotriazole-*N,N,N′,N′*-tetramethyluronium hexafluoro-phosphate (HBTU), and 4-(2′,4′-dimethoxyphenyl-Fmoc-aminomethyl)-phenoxy resin (Rink amide resin LS, 100–200 mesh, 1% divinylbenzene [DVB] 0.2 mmol/g) were from Advanced Chemtech. Pyridine, acetic anhydride, acetic acid, and anhydrous ether were from J.T. Baker. Triisopropylsilane, *N,N′*-diisopropylethylamine, and 1,2-ethanedithiol were purchased from Sigma-Aldrich. High-performance liquid chromatography (HPLC)–grade acetonitrile (CH_3CN) and Millipore 18-mΩ water were used for peptide purifications. SFB was purchased from ABX GmbH. All other standard synthesis reagents were purchased from Sigma-Aldrich Chemical Co. All the other general materials (cell lines, mice, etc.) and instruments (reversed-phase

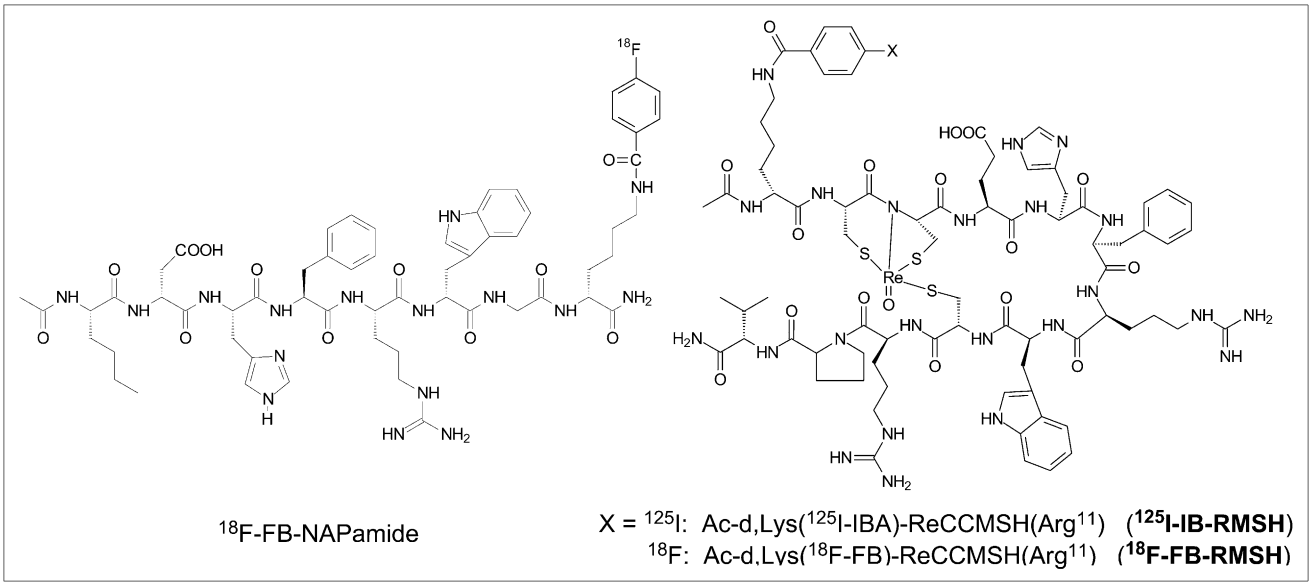

FIGURE 1. Schematic structures of ^{18}F-FB-NAPamide, ^{125}I-IB-RMSH, and ^{18}F-FB-RMSH.

HPLC, radioactive dose calibrator, and electrospray ionization mass spectrometry [ESI-MS] or matrix-assisted laser desorption/ionization time-of-flight mass spectrometry [MALDI-TOF-MS]) are the same as previously reported (*11*).

Synthesis of RMSH

Ac-D-Lys-CCMSH(Arg^{11}) (amino acid sequence, Ac-kCCEHdFRWCRPV-NH_2) was synthesized using conventional Fmoc/HBTU peptide synthesis chemistry. RMSH was then prepared by rhenium coordination using a transchelation reaction with rhenium-glucoheptonate as previously described (*14,19*). The resulting rhenium-chelated RMSH was purified by a semipreparative gradient HPLC system with a C-18 column. Ultraviolet detection wavelengths were 218, 254, 280, and 412 nm for all experiments. The flow rate was 3 mL/min, with the mobile phase starting with 15%:85% solvent B to solvent A (0–3 min), then increasing to 20%:80% solvent B to solvent A at 33 min and 85%:15% solvent B to solvent A at 36 min, and being maintained at this composition for another 3 min (36–39 min). The gradient returned to the initial solvent composition by 42 min from the start of injection. Fractions containing the product were collected and lyophilized. Peptide identities were confirmed by ESI-MS or MALDI-TOF-MS.

$^{18/19}$F-SFB Conjugation with RMSH

The reference standard ^{19}F-FB-RMSH was prepared by reaction of RMSH with SFB (*19*). Briefly, RMSH and SFB dissolved in dimethyl sulfoxide (100 μL) and *N,N′*-diisopropylethylamine (5 μL) were mixed and reacted for 1 h at 50°C. The reaction solution was quenched by adding TFA (50 μL) and injected into a semipreparative HPLC column for purification. The flow rate was 3 mL/min, with the mobile phase starting at 95% solvent A and 5% solvent B (0–3 min), going to 35% solvent A and 65% solvent B at 33 min, then going to 15% solvent A and 85% solvent B, and being maintained at this solvent composition for another 3 min (36–39 min). The gradient returned to the initial solvent composition by 42 min. Fractions containing the product were collected, lyophilized, and characterized by ESI-MS or MALDI-TOF-MS.

The radiofluorination synthon ^{18}F-SFB was prepared using a procedure reported previously (*11,23*). ^{18}F-SFB (specific activity, 5.4–6.8 Ci/μmol, or 200–250 GBq/μmol) dissolved in acetonitrile (100 μL) was added to the RMSH peptide (100 μg) dissolved in Na_2HPO_4 buffer (900 μL, pH 8.0) and reacted for 1 h at 60°C. After TFA (50 μL) had been added to quench the reaction, the reaction solution was injected into a semipreparative HPLC column using the same elution gradient as the one used in the synthesis of cold ^{19}F-FB-RMSH. The HPLC fractions containing the radiolabeled product were subsequently collected, combined, and evaporated with a rotary evaporator to dryness. The radiolabeled peptide was reconstituted in phosphate-buffered saline (PBS) and passed through a 0.22-μm Millipore filter into a sterile vial for in vitro and animal experiments.

In Vitro Cell Binding Assay

B16/F10 murine melanoma cells and A375M cells were cultured in Dulbecco's modified Eagle's high-glucose medium supplemented with 10% fetal bovine serum and penicillin and streptomycin. The cells were maintained in a 37°C, 5% CO_2 humidified incubator. The receptor binding affinity studies of RMSH and ^{19}F-FB-RMSH for the MC1R were performed using B16F10 cells. Briefly, 0.5 × 10^6 cells were resuspended in Dulbecco's modified Eagle's medium containing 25 mM *N*-(2-hydroxyethyl)piperazine-*N′*-(2-ethanesulfonic acid), 0.2% bovine serum albumin, and 0.3 mM 1,10-phenanthroline. The cells were then incubated at 37°C for 90 min with either RMSH or ^{19}F-FB-RMSH (peptide concentration varying from 10^{-12} to 10^{-6} M) and approximately 200,000 counts per min of ^{125}I-(Tyr^2)-[Nle^4,D-Phe^7]–α-MDP (NDP). Cells were washed 3 times with ice-cold PBS, and the radioactivity of the cells was measured. Data were analyzed using GraphPad Prism 5.0 (GraphPad Software), and the IC_{50} values, the concentration of competitor required to inhibit 50% of the radioligand binding, of the peptides were calculated.

Biodistribution Studies

All animal experiments were performed in compliance with a protocol approved by Stanford University Institutional Animal Care and Use Committee. Five- to 6-wk-old male C57BL/6 mice were implanted with 1 × 10^6 B16F10 murine melanoma cells and Foxn1 nude mice (5–6 wk old) were inoculated with 3 × 10^6 A375M human melanoma cells in the right shoulder. When the diameters of the tumors reach around 8 mm, approximately 1.11 MBq (30 μCi) of ^{18}F-FB-RMSH was injected into each mouse through the tail vein. For a blocking study, another group of B16F10 tumor–bearing mice (n = 2) was coinjected with 250 μg of unlabeled NDP peptide (Sigma-Aldrich) in PBS containing 2% bovine albumin serum (Invitrogen). After the injection of the radiotracer, the B16/F10 mice (n = 3) were sacrificed at 1, 2, and 4 h after injection, and the A375M (n = 3) and blocking group B16F10 mice were sacrificed at 2 h after injection. Tumors, blood, and major organs of interest were harvested, weighed, and counted in a Wallac 1480 automated γ-counter (Perkin Elmer). These results were expressed as %ID/g.

Small-Animal PET Studies

PET of tumor-bearing mice was performed on a small-animal PET R4 rodent model scanner (Siemens Medical Solutions USA, Inc.). The mice bearing B16F10 or A375M tumors were injected with 1.28–1.64 MBq (34.7–44.4 μCi) of ^{18}F-FB-RMSH via the tail vein. At 1 and 2 h after injection, the mice were anesthetized with 2% isofluorane and placed prone near the central field of view in the scanner. The 5-min static scans were obtained, and the images were reconstructed by a 2-dimensional ordered-subsets expectation maximum algorithm. Regions of interest (ROIs) were then drawn over the tumor or organ of interest on decay-corrected whole-body coronal images. The mean counts per pixel per minute were obtained from the ROI and converted to counts per milliliter per min using a calibration constant. By assuming a tissue density of 1 g/mL, we converted the ROIs to counts/g/min. An image ROI-derived %ID/g of tissue was then determined by dividing counts per gram per minute with injected dose. No attenuation correction was performed.

Western Blot

Tumor lysate was prepared by homogenizing tumor specimens in a radioimmunoprecipitation assay buffer (Sigma). The supernatant was collected by centrifugation at 14,000 rpm for 10 min at 4°C. The protein concentrations of the samples were measured using the Bradford assay (BioRad). An equal amount of protein from each sample was loaded onto a 10% NuPAGE Bis-Tris gel and electroblotted to a polyvinylidene fluoride membrane. After blocking with Tris-buffered saline and 0.05% polysorbate 20 containing 5% powdered milk, the membrane was incubated

overnight with monoclonal anti-MC1R antibody L-20 and N-19 (Santa Cruz Biotechnology) (1:500), followed by incubation with the horseradish peroxidase–conjugated rabbit anti-goat IgG (Jackson ImmunoResearch) (1:5,000) for 1 h. After extensive washing, the protein bands were visualized using ECL Plus (Invitrogen). For determining the relative MC1R protein level, the intensity of the MC1R protein band was normalized with the intensity of the β-actin (Sigma-Aldrich) protein band from each sample.

Statistical Methods

Statistical analysis was performed using the Student *t* test for unpaired data. A 95% confidence level was chosen to determine the significance between groups, with *P* less than 0.05 being significantly different.

RESULTS

$^{19/18}$F-FB-RMSH Synthesis and IC_{50}

The linear peptide Ac-D-Lys-CCMSH(Arg^{11}) was first prepared using conventional solid-phase peptide synthesis methods. Further reaction of the linear peptide with the rhenium-glucoheptonate generated 2 major products, revealed by HPLC analysis (pk1 and pk2 in Fig. 2; gradient, 15%−20% over 30 min). The retention times on semipreparative HPLC for these 2 peaks were 23.7 and 26.6 min. Thus, the pure products could be obtained with chemical purity over 95%. Further MALDI-TOF-MS analysis showed that these peaks had the same molecular weight (MW) (within detection error range; Table 1). The isotopic pattern of the 2 products observed in the MALDI-TOF-MS spectra was also exactly the same. These data suggested that the 2 isolated rhenium-cyclized products were 2 different isomers, and thus, they were named RMSH-1 and RMSH-2, respectively. Each of these 2 isomers was further incubated in water for 17 h at 37°C; both rhenium complexes remained intact, as verified by HPLC. Decomposition and interchange between these 2 isomers were not observed. Interestingly, RMSH-1 exhibited higher binding affinity than did RMSH-2 on the basis of the competitive receptor binding assays (IC_{50} value, 5.4 vs. 13.9, as shown in Table 1).

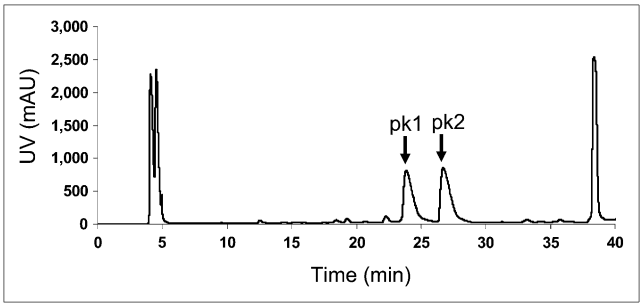

FIGURE 2. HPLC chromatogram of rhenium cyclization of Ac-D,Lys-CCMSH(Arg^{11}) reaction. Two isomers (RMSH-1 and -2) were separated. pk 1 = RMSH-1; pk 2 = RMSH-2; uv = ultraviolet.

TABLE 1. IC_{50} Values of α-MSH Analogs and Their Expected and Measured MW for $[M+H]^+$ by ESI-MS or MALDI-TOF-MS

Peptides	Expected	Measured	IC_{50} (nM)
Ac-D,Lys-CCMSH (Arg^{11})	1,605.9	1,605.6	ND
RMSH-1	1,804.1	1,803.7	5.4 ± 0.7
RMSH-2	1,804.1	1,804.7	13.9 ± 1.4
^{19}F-FB-RMSH-1	1,926.2	1,927.8	5.7 ± 0.7
^{19}F-FB-RMSH-2	1,926.2	1,928.2	9.0 ± 1.0

ND = not determined.

The nonradioactive fluorinated metallopeptides were then prepared by conjugation with cold SFB to allow for the characterization of the ^{18}F-labeled analogs of these peptides. Under the HPLC gradient (5%−65% over 30 min) used in the study, the retention times for RMSH-1 and -2 were both 17.8 min, and for their cold fluorinated counterparts, the times were 21.3 min. The desired products were purified by semipreparative HPLC (>90% yield and >95% purity) and characterized by MALDI-TOF-MS (Table 1). Receptor binding assay showed that the IC_{50} values of ^{19}F-FB-RMSH-1 and -2 were 5.7 and 9.0 nM, respectively.

Similarly, ^{18}F-FB-RMSH-1 and -2 were prepared by the conjugation of 2 RMSH-2 isomers with radioactive ^{18}F-SFB (specific activity, 200–250 GBq/μmol or 5.4–6.8 Ci/μmol). On the basis of the retention times acquired from the nonradioactive fluorinated peptides, the radiofluorinated products were collected and used for biologic evaluation using the same gradient HPLC method. The total radiosynthesis time for making the radiopeptide took about 3 h. The maximum overall radiochemical yield with decay correction was approximately 35% at the end of synthesis. The radiochemical purities of the labeled peptides were over 95%, as verified by analytic radio-HPLC. Because the difference in retention times of radiolabeled and unlabeled peptide was greater than 3.5 min, the radiofluorinated RMSH-1 and -2 were easily separated from their nonradiolabeled counterparts by HPLC. The specific activity of the two ^{18}F-labeled metallopeptides was determined to be similar to that of the starting ^{18}F-SFB (132–166 GBq/μmol, decay-corrected).

In Vivo Biodistribution of ^{18}F-FB-RMSH-1 and -2

The in vivo biodistribution studies of both ^{18}F-FB-RMSH-1 and ^{18}F-FB-RMSH-2 were examined in B16F10 murine allograft– and A375M human xenograft melanoma–bearing mice. As shown in Table 2, for ^{18}F-FB-RMSH-1, the uptake in B16F10 tumor with high expression of MC1R was 1.97 ± 0.39, 2.11 ± 0.12, and 0.83 ± 0.05 %ID/g at 1, 2, and 4 h, respectively, after injection, suggesting good tumor uptake and retention of this PET probe. ^{18}F-FB-RMSH-1 also displayed rapid blood clearance and low uptake in muscle, resulting in decent tumor-to-blood and

TABLE 2. Biodistribution Data for ^{18}F-FB-RMSH-1 and -2 in C57BL/6 Mice Bearing Subcutaneously Xenotransplanted B16F10 Murine Melanoma and Foxn1 Nude Mice Bearing A375M Human Melanoma

	^{18}F-FB-RMSH-1					^{18}F-FB-RMSH-2	
	B16F10						
Organ	1 h	2 h	4 h	B16F10 block (2 h)	A375M (2 h)	B16F10 (2 h)	A375M (2 h)
Tumor	1.97 ± 0.39	2.11 ± 0.12	0.83 ± 0.05	1.62 ± 0.11	0.33 ± 0.04	1.36 ± 0.18	0.42 ± 0.19
Blood	1.98 ± 0.57	0.76 ± 0.19	0.39 ± 0.18	1.21 ± 0.05	0.43 ± 0.02	0.40 ± 0.07	0.25 ± 0.05
Heart	1.30 ± 0.44	0.62 ± 0.15	0.33 ± 0.12	0.76 ± 0.03	0.56 ± 0.17	0.30 ± 0.03	0.22 ± 0.03
Liver	5.62 ± 2.14	2.45 ± 0.45	1.15 ± 0.37	4.36 ± 0.63	1.35 ± 0.07	3.70 ± 0.63	2.92 ± 0.45
Lung	6.42 ± 2.50	2.39 ± 0.62	1.32 ± 0.40	4.00 ± 0.71	1.75 ± 0.17	1.22 ± 0.12	1.16 ± 0.20
Muscle	0.61 ± 0.11	0.27 ± 0.07	0.17 ± 0.04	0.40 ± 0.08	0.21 ± 0.01	0.21 ± 0.02	0.19 ± 0.09
Spleen	1.32 ± 0.48	0.81 ± 0.29	0.28 ± 0.04	0.53 ± 0.13	0.54 ± 0.07	0.74 ± 0.18	0.46 ± 0.07
Brain	0.14 ± 0.06	0.08 ± 0.01	0.04 ± 0.01	0.06 ± 0.00	0.04 ± 0.00	0.04 ± 0.01	0.03 ± 0.00
Intestine	1.28 ± 0.44	0.95 ± 0.35	0.68 ± 0.37	2.70 ± 0.46	0.44 ± 0.07	0.47 ± 0.09	0.78 ± 0.72
Stomach	2.33 ± 0.60	0.82 ± 0.29	0.52 ± 0.19	1.86 ± 0.23	0.41 ± 0.05	0.41 ± 0.07	0.31 ± 0.13
Pancreas	0.66 ± 0.18	0.24 ± 0.08	0.28 ± 0.18	0.41 ± 0.06	0.19 ± 0.04	0.11 ± 0.03	0.10 ± 0.01
Bone	1.32 ± 0.35	0.83 ± 0.10	0.30 ± 0.07	1.40 ± 0.91	0.46 ± 0.04	0.36 ± 0.20	0.30 ± 0.15
Kidney	7.72 ± 1.19	5.42 ± 0.50	5.09 ± 1.07	9.81 ± 0.25	5.02 ± 0.10	17.8 ± 1.80	16.86 ± 2.93
Uptake ratio							
Tumor to blood	1.01 ± 0.08	2.59 ± 0.26	1.65 ± 0.11	1.48 ± 0.10	0.77 ± 0.14	3.49 ± 0.92	1.98 ± 1.16
Tumor to muscle	3.24 ± 0.06	7.43 ± 0.81	5.24 ± 1.43	3.13 ± 0.74	1.57 ± 0.26	7.01 ± 2.95	2.53 ± 1.19

Data are mean ± SD %ID/g after intravenous injection of 1.28–1.64 MBq (34.7–44.4 μCi) of tracer (n = 3).

tumor-to-muscle ratios (2.59 ± 0.26 and 7.43 ± 0.81, respectively) at 2 h after injection. Also, ^{18}F-FB-RMSH-1 displayed moderate uptake in the lungs (Table 2). Finally, relatively high uptake in the kidneys and moderate uptake in the liver were also observed for ^{18}F-FB-RMSH-1 in B16F10 tumor–bearing mice. The level of accumulation in the kidney and liver, respectively, was 7.72 ± 1.19 and 5.42 ± 0.50 %ID/g at 1 h after injection, and it dropped to 5.09 ± 1.07 and 1.15 ± 0.37 %ID/g at 4 h after injection. For the A375M model, tumor uptake of ^{18}F-FB-RMSH-1 was only 0.33 ± 0.04 %ID/g at 2 h after injection, which was significantly lower than uptake in B16/F10 tumors ($P < 0.01$). A lower tumor–to–normal organ ratio was also observed in the A375M model, with only 0.77 ± 0.14 for the tumor-to-blood ratio and 1.57 ± 0.26 for the tumor-to-muscle ratio ($P < 0.01$). With NDP coinjection, ^{18}F-FB-RMSH-1 had a reduced tumor uptake (1.62 ± 0.11 %ID/g) at 2 h after injection, with the tumor-to-blood ratio reduced to 1.48 ± 0.10 (Table 2).

For ^{18}F-FB-RMSH-2, the uptake in the B16F10 tumor model was 1.36 ± 0.18 %ID/g at 2 h after injection, which was much lower than that of ^{18}F-FB-RMSH-1 ($P < 0.05$) (Table 2). However, lower blood activity was seen for this probe, which led to a little bit higher tumor-to-blood ratio than that for its ^{18}F-labeled isomer (3.49 ± 0.92 vs. 2.59 ± 0.26 %ID/g) ($P > 0.05$). Interestingly, ^{18}F-FB-RMSH-2 showed more than a 3-fold higher kidney uptake than its isomer at 2 h after injection ($P < 0.05$). In addition, ^{18}F-FB-RMSH-2 demonstrated higher uptake in the liver but lower uptake in the lung than did ^{18}F-FB-RMSH-1. For most other normal organs, ^{18}F-FB-RMSH-2 exhibited uptake similar to that of ^{18}F-FB-RMSH-1. For the A375M model, ^{18}F-FB-RMSH-2 revealed low tumor uptake (0.42 ± 0.19 %ID/g), but high tracer uptake (16.86 ± 2.93 %ID/g) was observed in the kidneys at 2 h after injection.

Small-Animal PET

Small-animal PET of mice bearing B16F10 using ^{18}F-FB-RMSH-1 and -2 was first compared (Fig. 3A). Visual examination showed that ^{18}F-FB-RMSH-1 uptake in tumors was higher than ^{18}F-FB-RMSH-2 uptake at both 1 and 2 h after injection. Both probes showed moderate to high uptakes in liver and kidney. Further quantification analysis of small-animal PET images demonstrated that ^{18}F-FB-RMSH-2 has a much higher uptake in kidney than that of ^{18}F-FB-RMSH-1 ($P < 0.01$) at 1 and 2 h after injection (Figs. 3C and 3D). Improved quality of PET images was also observed at 2 h after injection for ^{18}F-FB-RMSH-1. On the basis of these findings, isomer ^{18}F-FB-RMSH-1 was selected as a PET probe for further evaluation and imaging studies.

^{18}F-FB-RMSH-1 was then imaged in the nude mice bearing A375M melanoma with low MC1R expression at 1 and 2 h (Fig. 3B). Compared with B16F10 tumor–bearing mice, much lower tumor uptake and poor tumor-to-background ratio was observed in A375M tumors at both time points. The A375M tumor was barely discernable, particularly at 2 h after injection, whereas high activity accumulation in the kidneys was still observed.

Western Blot

The expression of MC1R in B16F10 and A375M tumors was further confirmed by Western blot analysis (Fig. 4). B16F10 tumors were confirmed to have high MC1R expression, whereas the opposite was observed for the A375M tumors, which is consistent with the radioactive

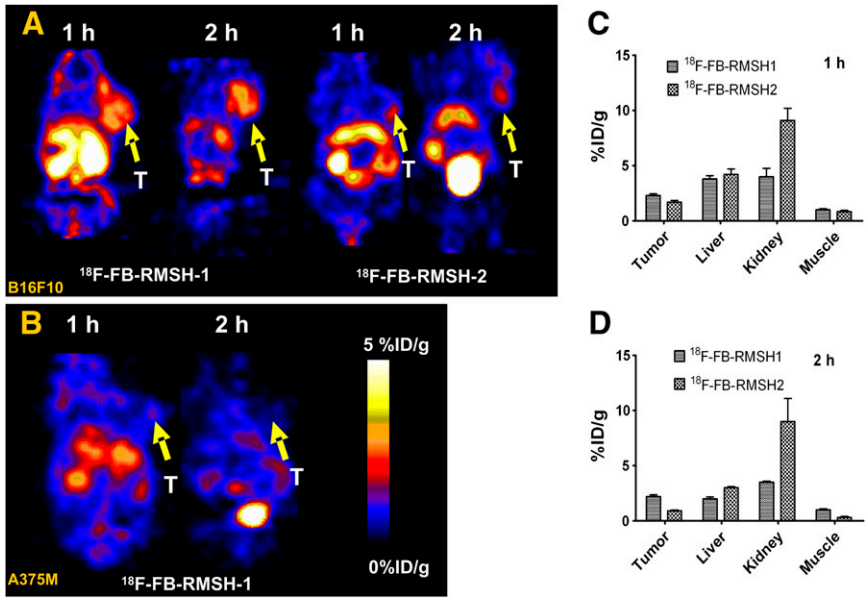

FIGURE 3. (A) Representative decay-corrected coronal small-animal PET images of mice bearing B16F10 tumors on right shoulder at 1 and 2 h after tail vein injection of ^{18}F-FB-RMSH-1 (left) and -2 (right) (n = 3 for each group). (B) Representative decay-corrected coronal small-animal PET images of A375M tumor–bearing mice at indicated time points after tail vein injection of ^{18}F-FB-RMSH-1. (C and D) Tumor and other normal organ uptakes and ratios derived from 1 and 2 h after tail vein injection of ^{18}F-FB-RMSH-1 or -2. Arrows indicate locations of tumors (T). Data are shown as mean ± SD %ID/g (n = 3).

binding assay reported previously (*12*). The relative band intensity was 18:1.

DISCUSSION

It has been reported that overexpression of MC1R may correlate with the prognosis of malignant melanoma. Several studies have been performed to design molecular probes that specifically target MC1R in melanoma. The major goal of this research was to radiofluorinate a promising MC1R-targeting peptide rhenium-cyclized CCMSH(Arg^{11}) analog and to further evaluate it as a PET probe for imaging malignant melanoma with different MC1R expression.

Two isomers of rhenium-cyclized Ac-D-Lys-CCMSH(Arg^{11}), RMSH-1 and -2, are reproducibly formed in this study. They could be separated by reversed-phase HPLC with different retention times (23.7 vs. 26.6 min, Fig. 2), whereas the same mass-to-charge ratio (m/z) value was obtained on the basis of mass spectroscopy. To the best of our knowledge, this is, so far, the first report on the observation of 2 isomers when rhenium is used to cyclize the peptides containing 3 cysteine residues. This observation is likely caused by different HPLC purification methods used in different studies. In the current study, the HPLC gradient used was 15%−20% over 30 min, whereas the gradient was 18%−28% over 20 min in our former publication on preparation of ^{125}I-IB-RMSH, which was steep and might not be able to separate 2 isomers. Both isomers possess high MC1R binding affinity in the nanomolar range. Further modification of RMSH with an SFB label slightly improved their affinities (Table 1). The high affinities of ^{19}F-FB-RMSH-1 and -2 were encouraging, justifying the further in vivo evaluation of the ^{18}F-FB-RMSH peptides.

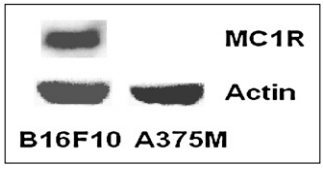

FIGURE 4. Western blot detection of MC1R expression in B16F10 (right) and A375M (left) tumor tissues. B16F10 or A375M tumor tissue homogenates were prepared, and 40 μg proteins were detected with goat antimouse (L-20) and goat antihuman (N-19) monoclonal MC1R antibody. (Top) MC1R. (Bottom) β-Actin.

In biodistribution studies with a B16F10 tumor model, higher tumor uptake was observed for ^{18}F-FB-RMSH-1 than for ^{18}F-FB-RMSH-2, and much lower kidney uptake for RMSH-1 at 2 h was observed. Although it is unknown what causes this dramatic difference, it highlights the importance of fine-tuning the structure of the rhenium-cyclized α-MSH peptide to achieve better radiotracer distribution and clearance. Similarly, the differences in tumor and major-organ uptake could also be observed for 2 isomers in vivo by small-animal PET studies, and the quantification of small-animal PET images showed a significant difference in both tumor and kidney uptake (P < 0.01) (Fig. 3C and 3D). ^{18}F-FB-RMSH-2 has a lower tumor uptake but higher kidney uptake at both 1 and 2 h. On the basis of these findings for the 2 different isomers of purified metallopeptides, ^{18}F-FB-RMSH-1 displayed more favorable properties, suggesting that it could become a better candidate for imaging MC1R in vivo. However, there is still around 5.42 ± 0.50 %ID/g kidney uptake and moderate lung and liver uptake at 2 h after injection (Table 2). The kidney uptake could be decreased by coinjection of basic compounds including lysine and arginine or plasma expander (*18,24–26*). The exact mechanism responsible for moderate lung uptake is not clear yet. It may be caused by the unique structure of the halogenated peptide cyclized by transition metal rhenium. Further studies are needed to

address this problem and optimize the in vivo behavior of the probe. Moreover, it is observed that the lung activity decreases in parallel with the liver activity, as is likely caused by the metabolism of the probe and subsequent excretion of radioactive metabolites through the liver and kidneys.

^{18}F-labeled NDP, which behaves differently from the cyclized metallopeptide, was reported to display high binding affinity to MC1R in vitro in a previous study (*27*). Several other radionuclides have been applied to rhenium-cyclized CCMSH as a scaffold in our previous studies (*15,19*). Iodinated ReCCMSH analogs exhibited a significantly higher tumor uptake and retention than did the iodinated linear peptide NDP (*19*). Recently, our group developed ^{18}F-FB-NAPamide as a PET probe to image MC1R in vivo expression (*11*). Although the binding affinity of ^{19}F-FB-NAPamide is high (IC_{50} = 7.2 nM), its tumor uptake and retention are suboptimal in the B16F10 model (*11*). In the current research, though, ^{18}F-FB-RMSH-1 showed a binding affinity similar to ^{18}F-FB-NAPamide (IC_{50}, 5.4 nM) and demonstrated higher tumor uptake and. The B16F10 uptake at 1 h is 1.97 ± 0.39 %ID/g (1.6-fold), with 42% of the radioactivity (0.83 ± 0.05 %ID/g) still remaining in the tumor at 4 h. These data demonstrated the advantages of using rhenium-cyclized CCMSH(Arg^{11}) as a scaffold for developing the MC1R PET agent, as proves our initial hypothesis. In addition, ^{18}F-FB-RMSH displayed much lower B16F10 tumor and blood uptake than that of the ^{125}I-labeled counterpart in the B16F1 tumor model, suggesting a high impact of the radiolabels on the in vivo behavior of the peptides.

In further ^{18}F-FB-RMSH-1 PET studies, B16F10 tumors are clearly delineated over the background at 1 and 2 h after injection; PET quantification analysis also confirms good tumor retention of the probe—retention that is different from the patterns displayed in the liver, kidney, and muscle (Fig. 3A). This increased tumor residence time would allow the characterization of specific malignant melanoma patients with MC1R expression. For the A375M tumor model, the tumors are slightly noticeable at 1 h, probably because of nonspecific uptake. This is evidenced by poor A375M tumor imaging at 2 h after injection (Fig. 3B). The much higher tumor uptake and tumor-to-background ratio in the B16F10 model than that in the A375M model are consistent with the finding obtained from the biodistribution studies. Furthermore, the better PET quality in B16F10 tumor than that in the A375M also suggests that ^{18}F-FB-RMSH-1 could differentiate melanoma with different MC1R expression in living subjects. Compared with ^{18}F-FB-NAPamide–based PET images (*11*), ^{18}F-FB-RMSH-1 also shows good tumor uptake and good tumor-to-background contrast in B16F10 tumor–bearing mice but no uptake in A375M tumor–bearing mice. Although the tumor uptake is lower for ^{18}F-FB-NAPamide, higher liver and kidney uptake were observed for ^{18}F-FB-RMSH-1 and -2 at 1 h after injection. Further optimization will be needed for both linear and cyclized PET probes targeting MC1R for translational purposes.

CONCLUSION

The rhenium-cyclized α-MSH analogs ^{18}F-FB-RMSH-1 and -2 were successfully prepared, and their characteristics including binding affinities and in vivo distribution were elucidated in this study. ^{18}F-FB-RMSH-1 demonstrates significant advantages as a probe over ^{18}F-FB-RMSH-2. ^{18}F-FB-RMSH-1 displays good uptake and retention in MC1R-overexpressing tumors and is a promising PET probe for imaging MC1R-positive melanoma and MC1R expression in vivo.

ACKNOWLEDGMENTS

This work was supported, in part, by grant R24 CA93862 from the National Cancer Institute (NCI) Small Animal Imaging Resource Program (SAIRP) and grant P50 CA114747 from the NCI *In Vivo* Cellular Molecular Imaging Center (ICMIC).

REFERENCES

1. Jemal A, Siegel R, Ward E, Hao Y, Xu J, Thun MJ. Cancer statistics, 2009. *CA Cancer J Clin.* 2009;59:225–249.
2. Gray-Schopfer V, Wellbrock C, Marais R. Melanoma biology and new targeted therapy. *Nature.* 2007;445:851–857.
3. Belhocine TZ, Scott AM, Even-Sapir E, Urbain JL, Essner R. Role of nuclear medicine in the management of cutaneous malignant melanoma. *J Nucl Med.* 2006;47:957–967.
4. Choi EA, Gershenwald JE. Imaging studies in patients with melanoma. *Surg Oncol Clin N Am.* 2007;16:403–430.
5. Dimitrakopoulou-Strauss A, Strauss LG, Burger C. Quantitative PET studies in pretreated melanoma patients: a comparison of 6-[^{18}F]fluoro-L-dopa with ^{18}F-FDG and ^{15}O-water using compartment and noncompartment analysis. *J Nucl Med.* 2001;42:248–256.
6. Cobben DC, Jager PL, Elsinga PH, Maas B, Suurmeijer AJ, Hoekstra HJ. 3′-^{18}F-fluoro-3′-deoxy-L-thymidine: a new tracer for staging metastatic melanoma? *J Nucl Med.* 2003;44:1927–1932.
7. Decristoforo C, Hernandez Gonzalez I, Carlsen J, et al. ^{68}Ga- and ^{111}In-labelled DOTA-RGD peptides for imaging of αvβ3 integrin expression. *Eur J Nucl Med Mol Imaging.* 2008;35:1507–1515.
8. Siegrist W, Solca F, Stutz S, et al. Characterization of receptors for α-melanocyte-stimulating hormone on human melanoma cells. *Cancer Res.* 1989;49:6352–6358.
9. Siegrist W, Stutz S, Eberle AN. Homologous and heterologous regulation of α-melanocyte-stimulating hormone receptors in human and mouse melanoma cell lines. *Cancer Res.* 1994;54:2604–2610.
10. McQuade P, Miao Y, Yoo J, Quinn TP, Welch MJ, Lewis JS. Imaging of melanoma using ^{64}Cu- and ^{86}Y-DOTA-ReCCMSH(Arg^{11}), a cyclized peptide analogue of α-MSH. *J Med Chem.* 2005;48:2985–2992.
11. Cheng Z, Zhang L, Graves E, et al. Small-animal PET of melanocortin 1 receptor expression using a ^{18}F-labeled α-melanocyte-stimulating hormone analog. *J Nucl Med.* 2007;48:987–994.
12. Cheng Z, Xiong Z, Subbarayan M, Chen X, Gambhir SS. ^{64}Cu-labeled α-melanocyte-stimulating hormone analog for microPET imaging of melanocortin 1 receptor expression. *Bioconjug Chem.* 2007;18:765–772.
13. Miao Y, Hoffman TJ, Quinn TP. Tumor-targeting properties of ^{90}Y- and ^{177}Lu-labeled α-melanocyte stimulating hormone peptide analogues in a murine melanoma model. *Nucl Med Biol.* 2005;32:485–493.
14. Cheng Z, Chen J, Miao Y, Owen NK, Quinn TP, Jurisson SS. Modification of the structure of a metallopeptide: synthesis and biological evaluation of ^{111}In-labeled DOTA-conjugated rhenium-cyclized α-MSH analogues. *J Med Chem.* 2002;45:3048–3056.

15. Chen J, Cheng Z, Hoffman TJ, Jurisson SS, Quinn TP. Melanoma-targeting properties of ^{99m}technetium-labeled cyclic α-melanocyte-stimulating hormone peptide analogues. *Cancer Res.* 2000;60:5649–5658.
16. Cheng Z, Mahmood A, Li H, Davison A, Jones AG. [^{99m}TcOAADT]-$(CH2)_2$-NEt2: a potential small-molecule single-photon emission computed tomography probe for imaging metastatic melanoma. *Cancer Res.* 2005;65:4979–4986.
17. Miao Y, Figueroa SD, Fisher DR, et al. ^{203}Pb-labeled α-melanocyte-stimulating hormone peptide as an imaging probe for melanoma detection. *J Nucl Med.* 2008;49:823–829.
18. Froidevaux S, Calame-Christe M, Tanner H, Eberle AN. Melanoma targeting with DOTA-α-melanocyte-stimulating hormone analogs: structural parameters affecting tumor uptake and kidney uptake. *J Nucl Med.* 2005; 46:887–895.
19. Cheng Z, Chen J, Quinn TP, Jurisson SS. Radioiodination of rhenium cyclized α-melanocyte-stimulating hormone resulting in enhanced radioactivity localization and retention in melanoma. *Cancer Res.* 2004;64:1411–1418.
20. Froidevaux S, Calame-Christe M, Tanner H, Sumanovski L, Eberle AN. A novel DOTA-α-melanocyte-stimulating hormone analog for metastatic melanoma diagnosis. *J Nucl Med.* 2002;43:1699–1706.
21. Chen J, Cheng Z, Owen NK, et al. Evaluation of an ^{111}In-DOTA-rhenium cyclized α-MSH analog: a novel cyclic-peptide analog with improved tumor-targeting properties. *J Nucl Med.* 2001;42:1847–1855.
22. Giblin MF, Wang N, Hoffman TJ, Jurisson SS, Quinn TP. Design and characterization of α-melanotropin peptide analogs cyclized through rhenium and technetium metal coordination. *Proc Natl Acad Sci USA.* 1998;95:12814–12818.
23. Zhang X, Xiong Z, Wu Y, et al. Quantitative PET imaging of tumor integrin $\alpha_v\beta_3$ expression with ^{18}F-FRGD2. *J Nucl Med.* 2006;47:113–121.
24. Miao Y, Fisher DR, Quinn TP. Reducing renal uptake of ^{90}Y- and ^{177}Lu-labeled α-melanocyte stimulating hormone peptide analogues. *Nucl Med Biol.* 2006;33: 723–733.
25. van Eerd JE, Vegt E, Wetzels JF, et al. Gelatin-based plasma expander effectively reduces renal uptake of ^{111}In-octreotide in mice and rats. *J Nucl Med.* 2006;47: 528–533.
26. Gotthardt M, van Eerd-Vismale J, Oyen WJ, et al. Indication for different mechanisms of kidney uptake of radiolabeled peptides. *J Nucl Med.* 2007; 48:596–601.
27. Vaidyanathan G, Zalutsky MR. Fluorine-18-labeled [Nle^4,D-Phe^7]-α-MSH, an α-melanocyte stimulating hormone analogue. *Nucl Med Biol.* 1997;24: 171–178.